Accelerated weathering of textile waste nonwovens used as sustainable agricultural mulching

**Houcine Abidi[1] ⬤, Sohel Rana[2], Walid Chaouch[1],
Bechir Azouz[1], Imed Ben Aissa[3], Mohamed Ben Hassen[1,4]
and Raul Fangueiro[5]**

Abstract

The removal of agriculture residual plastic films is nowadays a big concern for all environmentalists. Several ecological alternatives were developed for more sustainable products and cleaner production. In this work, the effect of three months of exposure under accelerated weathering conditions (ultraviolet light, moisture, and heat) on the properties of two textile waste nonwovens as a sustainable alternative to plastic mulching films was investigated. Results showed that thermostability and mechanical properties of the clothing textile waste felt and cotton waste nonwoven decreased after accelerated weathering. The chemical variation of cotton waste nonwoven and textile waste felt and the degradation rate of natural and synthetic fibers due to the photolysis and hydrolysis caused by accelerated weathering conditions were studied following the Fourier transform infrared spectroscopy and the fibrous composition variation of the blended textile waste felt structure during the study.

[1]Laboratory of Textile Engineering, Higher Institute of Technological Studies, University of Monastir, Ksar-Hellal, Tunisia
[2]Department of Chemical Sciences, School of Applied Sciences, University of Huddersfield, Huddersfield, UK
[3]Irrigation & Plant-Water Relations, Research Centre of Horticulture and Biological Agriculture, Sousse, Tunisia
[4]Department of Industrial Engineering, College of Engineer, Taibah University, Madina, Saudi Arabia
[5]Centre for Textile and technology, University of Minho, GuimarûÈes, Portugal

Corresponding author:
Mohamed Ben Hassen, College of Engineering: Industrial Engineering Department, Taibah University, Saudi Arabia.
Email: benrayen@yahoo.fr

Introduction

Textile fibers, since their discovery, were mainly used for clothing applications. But with the technological development, these materials became more used in a wide variety of technical applications (automotive and aeronautics, medical and hygiene applications, protection and defense, civil and agricultural engineering...) and their use keeps growing continuously [1]. In the agricultural field, the use of technical textiles showed a promising development which led to the birth of new textile-based materials called agrotextiles [2]. The design of these agrotextiles could give knitted, woven, or nonwoven textile structures according to the final product requirement. The use of textiles in agricultural field is increasing worldwide which inquires a growing production rate and a wide range of products. Agrotextiles production volume represented 8.2% of the global technical textiles market in 2010. This sector will be among the strongest growth predictions based on the increase of food production that will be 70% higher than the current level and the increase of global population which will exceed nine billion by 2050 [3]. The agrotextiles are used in crop's production, animal husbandry, horticulture, floriculture, aqua culture, and agro-engineering applications [4,5]. The destination of the products defines the type of materials that should be used in agrotextiles manufacturing. Among the most common agrotextiles, we find the mulching films or mats used to cover the soil. The mulching films are basically used to increase crop yield and improve its quality, control the weeds growth, reduce the use of chemical pesticides, reduce the volume of water irrigation, keep the soil moisture, and increase its temperature [6]. The mulching films are mainly made from low-density polyethylene due to their fastness to weather conditions, their resistance to microorganisms, and their low cost. The market of plastic mulching films accounted 40% of the global volume of agricultural plastic films and is expected to grow with an annual rate of 7.6% from 2013 to 2019 [7]. Despite its growth, the main disadvantage of plastic mulching films is the handling of their wastes which are mainly landfilled or incinerated since they are contaminated with soil and the recycling cost could be high. The plastic residue deteriorates the soil and decreases its fertility [8]. For these reasons, the researchers developed several bioplastics and biodegradables plastics to avoid the treatment of the end-of-life plastic waste. The biodegradable plastics could be a promising alternative for polyethylene plastic currently used for mulching applications since it improves soil temperature, moisture, and crop yield [9], but several parameters should be improved, mainly the high cost, the control of biodegradability, and a series of rigorous studies are still required to ensure its safe use and to measure the real environmental impact of its long-term accumulation, after degradation, on the soil, on the atmosphere or on the aquatic environment [7]. The environment considerations and the waste treatment constraints incited the researchers

to evaluate the potential of natural fibers in agricultural applications and find an ecological alternative for polluting plastic products. Thanks to their biodegradable aspect, the natural fibers were used in different agrotextiles manufacturing [10] including mulching applications. Wool, cotton, palm leaves, bagasse, flax, jute, Alfa, Agave, and coir fibers have been used to synthesize environmentally friendly mulching mats in order to substitute the plastic ones [11–19]. The natural fibers showed a huge potential to be used not only as mulching films but also in several agricultural applications thanks to their good mechanical properties, high moisture retention [20], and their renewable resources unlike petroleum-based materials. The advantages of agrotextiles based on natural fibers were not enough and their use remains limited comparing to plastic products which are cheaper, with lighter weight and longer life service [21]. Agrotextiles must satisfy user's requirements which are mainly the mechanical performances, weathering resistance, and appropriate lifetime. The variation of agrotextiles properties during the time of use was studied in several research works. The degradation of agrotextiles under outdoor natural weathering conditions [22] or/and laboratory accelerated weathering conditions was investigated [23]. The influence of exposure time to ultraviolet (UV) light and water spray on the chemical changes and mechanical properties of biodegradable agrotextiles based on natural fibers such as wool were investigated in different works [11] or synthetic ones like polyethylene films [24]. The biodegradation due to microorganisms was also studied for single fibers [25] or textile structures such as cotton and polyester fabrics [26] to evaluate their performances in presence of microorganisms after being buried in the soil. Different techniques were used, and the most common was the quantification of the emitted amount of CO_2 during the biodegradation reaction. An appropriate lifetime and the resistance to different types of degradation are very important factors for the marketing of agrotextiles. Prosenjit Saha et al. [16] applied a chemical treatment to enhance the resistance of jute-based geotextiles and make their lifetime three to five times longer. The improvement of the antimicrobial activity is one of the functionalization techniques of agrotextiles that were also investigated by developing a hemp structure loaded with microcapsules showing a better resistance to microorganisms [27]. The agrotextiles are mainly made from raw materials to ensure good mechanical properties and high weathering resistance. However, with the development of recycling technologies, the use of recycled materials in agrotextiles manufacturing started to emerge for environmental reasons as well as economical interest [28]. In this work, the evaluation of agrotextiles issued from textile waste recycling industry (mono fiber and blended structures) was investigated because of the lack of researches regarding the textile wastes products valorized in agricultural applications. In the textile industry, the end-of-life products could be landfilled, incinerated, or recycled. The recycled textiles are mainly used in automotive stuffing, furniture padding, dampening, and thermal insulations materials in construction applications [29]. In agricultural field, the use of recycled textiles as a sustainable geotextile to substitute plastic ones covering the soil to avoid erosion or to control weeds growth was studied. A comparative study between the mechanical properties and the degradation rate of cotton waste

film versus the current polyethylene films used for mulching applications was conducted by Jun Luo et al. [12]. The cotton waste structures showed good mechanical properties and higher degradation rate in the soil, but their elasticity and opacity to light were lower than those of polyethylene films. In this paper, the degradation of textile structures coming from waste recycling was evaluated. The effect of the exposure time under accelerated weathering conditions (UV, moisture, and temperature) on the different properties of mulching mats based on cotton spinning wastes and clothing wastes was studied. The changes in mechanical and thermal properties, surface morphology, air permeability, and fibrous composition variation were investigated. Since degradation was due to UV irradiation and moisture attack, it was necessary to evaluate the degradation rate via weight loss as well as the conventional tensile properties. Fourier transform infrared (FTIR) spectroscopy was used to understand the chemical modification related to the degradation of different fibers molecular chains. The variation in fibrous composition of the blended structures during the exposure time was also done in order to quantify the amount of degradation rate for the different fibers constituting the blended structure. Differential scanning calorimetry (DSC) and thermogravimetric analysis (TGA) provided a method to follow the variation of thermal properties and the influence of exposure time under degradation conditions on the weight loss and on the different characterizing temperatures of the different structures as well as their corresponding enthalpies. Dynamic mechanical analysis (DMA) was also done to evaluate the influence of exposure time on storage modulus and the glass transition temperature.

Material and methods

Material

Three textile structures were used for this study: A cotton nonwoven with a density of $200 \, g/m^2$ and a thickness of 2 mm and two non-woven felts composed from a blend of textile fibers with a density of $500 \, g/m^2$ and $700 \, g/m^2$ and a thickness of 7 and 10 mm, respectively. The felts were produced on cards and consolidated with a needling machine equipped with crown barb needles and a punch density of 36 punch/cm^2. A total of 1500 needles/m along 2.5 m working width with a stroke frequency of 350 strokes/min and a penetration needle depth reaching 3 mm were used for the consolidation of felts. Regarding the cotton nonwoven, the structures were needle punched with a punch density of 49 punch/cm^2, a stroke frequency of 150 strokes/min, and a penetration needle depth of 1 mm.

The samples were kindly donated, respectively, by SONIT SARL, Tunisia, and SOTRAFIB SARL, Tunisia and come both from the textile waste recycling industry: cotton spinning waste and textile clothing waste, respectively. For all the study, the cotton nonwoven fabric is referred as cotton waste nonwoven (CWNW) for CWNW and the felt is referred as textile waste felt (TWF) with TWF 500 and TWF 700 for TWF with, respectively, $500 \, g/m^2$ and $700 \, g/m^2$ of density. The characteristics of the samples used during this study are summarized in Table 1.

Table 1. Characteristics of samples used for the QUV degradation study.

Sample	Origin	Density (g/m^2)	Thickness range (mm)	Thickness average (mm)	Acronym
1	Textile clothing waste	500	5–10	6	TWF 500
2	Textile clothing waste	700	5–10	8	TWF 700
3	Cotton spinning waste	200	1–3	2	CWNW

CWNW: cotton waste nonwoven; TWF: textile waste felt.

Accelerating weathering tests

The samples were placed in a Q-Lab Ultra-Violet / Spray accelerated weathering tester according to ASTM D4355 about Deterioration of Geotextiles by exposure to light, moisture, and heat. The samples were exposed to alternating cycles of UV light and moisture under elevated temperature to simulate outdoor conditions of sunlight, dew, and rain. In this study, each 24-h weathering cycle consists of 12 h of UV light (Ultra-Violet A [UVA] 340 lamp with an irradiance equal to 76 W/m^2/nm) at 50°C and 12 h of water condensation at 40°C. The samples, with a size of 10×8 cm^2, were placed (in the machine direction (MD)) under these conditions for 2160 h and moved each day inside the QUV machine to ensure a homogenous repartition of UV light and moisture. The machine was calibrated each 400 h, and the UV irradiance was adjusted when needed.

Weight loss analysis

An analytical balance RADWAG AS220/C/2 was used to follow the variation of the weight loss of the different structures before and after the accelerated weathering.

The samples were taken out from the QUV machine each month and cleaned with ethanol/distilled water (70%/30%) to remove the particles fixed on the surface of specimen coming from its degradation or from the air. They were after dried at room temperature and then in oven at 105°C to remove moisture. The samples are cooled in a desiccator and then weighed [30].

Breaking force testing

The dynamometric tests were performed using a Dynamometer HOUNSFIELD H10KSMachine. The samples were subjected to the tensile tests at a constant speed of 25 mm/min, a load range of 50N, an extension range of 50 mm, and a gauge length equal to 25 mm. The tests were done according to the ASTM D5035 "Standard Test Method for Breaking Force and Elongation of Textile Fabrics (Strip Method)." For the reproducibility of the results, the test was replicated five times in the MD and the cross direction (CD), and the size of tested samples was 7.5 cm $\times$ 1.25 cm.

Thermal conductivity analysis

The thermal conductivity variation of the different structures under the effect of accelerated weathering was performed using a thermal conductivity meter Neotim FP2C and in accordance with ASTM D5930-97. Before conducting measurements, the samples were conditioned at standard textile conditions ($20°C \pm 2°C$, $65\% \pm 2\%$ Humidity Ratio [HR]) for 24 h. The average of three values was used to calculate mean values thermal conductivity for each sample.

Air permeability analysis

The air permeability before and after the aging tests was determined using Air Permeability Tester TEXTEST FX 3300 in accordance with ISO 9237. The samples were conditioned at standard textile conditions ($20°C \pm 2°C$, 65 % $\pm 2\%$ HR) for 24 h before the tests.

Quantitative fibrous composition analysis

The fibrous composition was determined using different chemical solvents specific for each type of fiber present in the blended structure. Referring to ISO 1833, ASTM D629-99 and the Portuguese Regulation (Diário da República, 1.a série—Nº 50—11 de Março de 2011), an experimental protocol was defined to dissolve the different fibers and determine the quantitative composition of the blended structures. The qualitative fibrous composition of the TWF was known in advance (indicated by the supplier), and the blended structure contains mainly polyester, cellulosic fibers, and protein fibers. To determine the percentage of each type of fiber, the fibers present in the blended structure were dissolved in a specific order according to their resistance to chemical solvents showed in Table 2.

Removal of nonfibrous constituents: The required starting weight for this study was 1 g. The specimen was first dried in an oven at 105°C for 5 h to remove the moisture and then removed and immediately cooled in desiccator over $CaSO_4$ before getting

Table 2. Dissolution of textile fibers in chemical solvents.

Fiber	Solvent		
	Sodium hydroxide	Sulfuric acid 75%	Sulfuric acid 100%
Protein fibers	S[*]	S	S
Cellulosic fibers	I[*]	S	S
PET	I	I	S

S*: soluble; I*: insoluble; PET: polyethylene terephthalate.

weighed. The dried specimen was then immersed in 150 mL of acetone for 2 h to remove the non-fibrous constituents, dried at room temperature to evaporate the acetone, and then dried in an oven at 105°C. The specimen was cooled in desiccator and then weighed.

Dissolution of protein fibers: After removing the non-fibrous constituents, the specimen was immersed in 150 mL of 5% sodium hypochlorite solution for 1 h at room temperature and stirred each 10 min. After, the specimen was washed under running tap water for 10 min and dried in an oven at 105°C, it was then cooled in desiccator and weighed.

Dissolution of cellulosic fibers: The cellulosic fibers were dissolved in diluted sulfuric acid solution. The specimen was immersed in 150 mL of 75% sulfuric acid, and the solution was heated at 50°C for 1 h. The solution was stirred each 10 min. The solution was decanted off, and the specimen was washed with cold water and ammonium hydroxide to neutralize the sulfuric acid. The specimen was after dried in an oven at 105°C and cooled in desiccator before being weighed.

Dissolution of polyester and synthetic fibers: The PET fibers were dissolved in concentrated sulfuric acid. The specimen was immersed in 150 mL of 95%–97% sulfuric acid at room temperature for 1 h. The solution was stirred each 10 min. The solution was decanted off, and the specimen was washed with cold water and ammonium hydroxide to neutralize the sulfuric acid. The specimen was then dried in an oven at 105°C, cooled in desiccator, and weighed.

FTIR spectroscopy

The FTIR spectra were obtained by FTIR SHIMADZU IRAffinity-1S with Horizontal Attenuated Total Reflectance HATR10 accessory and a resolution of 16 cm^{-1}. Forty-five scans were recorded with a wave length range between 4000 cm^{-1} and 700 cm^{-1} for each sample.

Differential scanning spectrometry

DSC analysis were performed in a DSC METTLER TOLEDO with a temperature range from 0°C to 500°C in nitrogen atmosphere (80 mL/min) and under a constant heating of 10°C/min. The weight of the sample should be between 5 and 10 mg. The mean values of three replicates were used.

Thermogravimetric analysis

TGA was performed in a STA Hitachi 7200 with a temperature range from 30°C to 600°C in nitrogen atmosphere (200 mL /min) and under a constant heating of 10°C/min. The weight of the sample should be between 5 and 10 mg.

Dynamic mechanical analysis

Dynamical experiments were carried out in a DMA Hitachi 7100 using Ben Dual Cantilever as a measurement mode. The heating rate was fixed at 3°C/min with a temperature range from 30°C to 150°C, and five different frequencies were set for all the samples (1, 2, 4, 10, and 20 Hz).

Results and discussions

Weight loss

The weight loss of the different structures under accelerated weathering conditions was studied during three months, and the results are shown in Figure 1.

Despite the limited exposure time, a degradation occurred for the different structures. The weight loss was not high (maximum of 7%) and the different structures showed a good resistance to UV and humidity cycles after three months of study. The weight loss was more significant for CWNW, made from cotton waste than that of TWF since the degradation of natural fibers was faster than synthetic fibers present in the blended TWF structures [31]. TWF 700 showed lower weight loss compared to TWF 500 and CWNW. The depth of penetration of UV light was an important factor influencing the degradation. The samples with higher packing density showed more resistance to UV light degradation due to less penetration of UV light and consequently, lower weight loss after three months of exposure to accelerated weathering conditions [32]. For the different structures, more than 50% of weight loss was obtained after the first month of accelerated weathering. The photodegradation started at the outer surface and penetrated gradually into the bulk of the material [33]. During the second month, the weight loss for TWF 500 and TWF 700 was minimal, and a plateau was observed showing that the degradation was slowed [34]. After the first step of photolysis in which the polymer backbone scissioned and the chain bonds broke, the degradation rate was retarded and the smaller constituents were more resistant [35]. For the CWNW samples, the
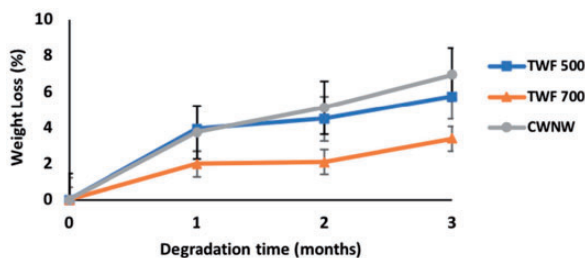

Figure 1. Weight loss versus degradation time under accelerated weathering. CWNW: cotton waste nonwoven; TWF: textile waste felt.

degradation rate was lower than the first month but stayed continuously increasing. Starting from the third month, the weight loss continued its increase for both structures but with a higher rate because of the beginning of the scission of short chains resulting from the initial step of degradation caused by accelerated weathering [36].

Breaking force

After three months of exposure to artificial weathering conditions of UV light, humidity, and heat, the tensile properties of textile waste nonwovens were investigated. The results of breaking force are shown in Figures 2 and 3 and elongation at break variation in Figures 4 and 5. The accelerated weathering conditions decreased the mechanical properties of mulching structures with different rates especially after the first month of exposure in both MD and CD [37]. The degradation was higher for the cotton based structure compared to blended structures since the degradation rate of natural fibers is higher than synthetic ones [31]. The CWNW lost more than 65% of breaking force after the first month and more than 85% after three months. The TWF showed more resistance to accelerated weathering conditions and lost around 50% of breaking force after three months. The CWNW showed higher breaking force values compared to TWF because its structure was reinforced by stitching throughout the MD during the production process. After the first month, the decrease in breaking force values was lower, and a plateau was observed for TWF curves.
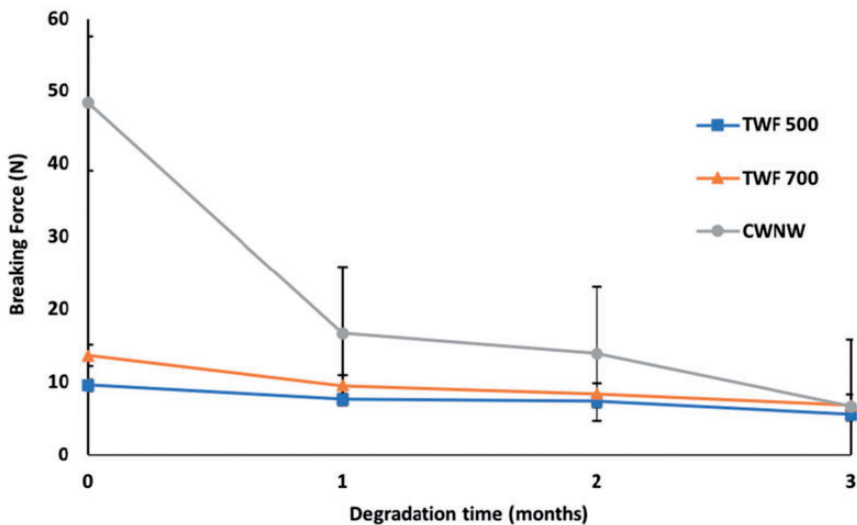

Figure 2. Breaking force versus degradation time under accelerated weathering in the machine direction. CWNW: cotton waste nonwoven; TWF: textile waste felt.
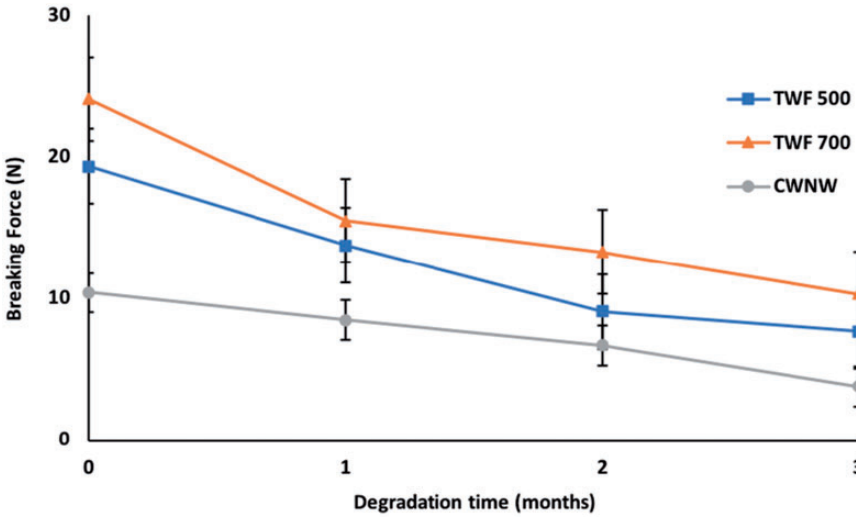
Figure 3. Breaking force versus degradation time under accelerated weathering in the cross direction. CWNW: cotton waste nonwoven; TWF: textile waste felt.
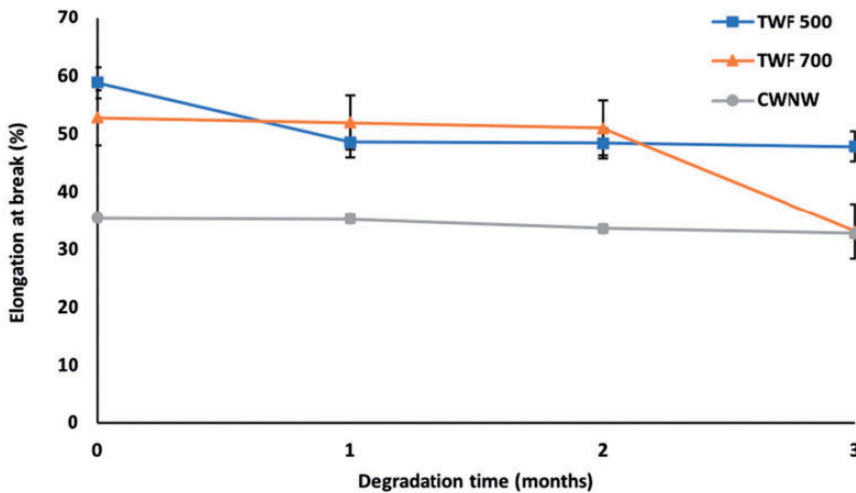

Figure 4. Elongation at break versus degradation time under accelerated weathering in the machine direction. CWNW: cotton waste nonwoven; TWF: textile waste felt.

The accelerated weathering conditions caused the opening of the supramolecular structure and the main chains scission resulting in shorter chains more resistant which could explain the slower degradation rate and the plateau observed in the breaking force curves [37]. This plateau was not seen for the CWNW, and the
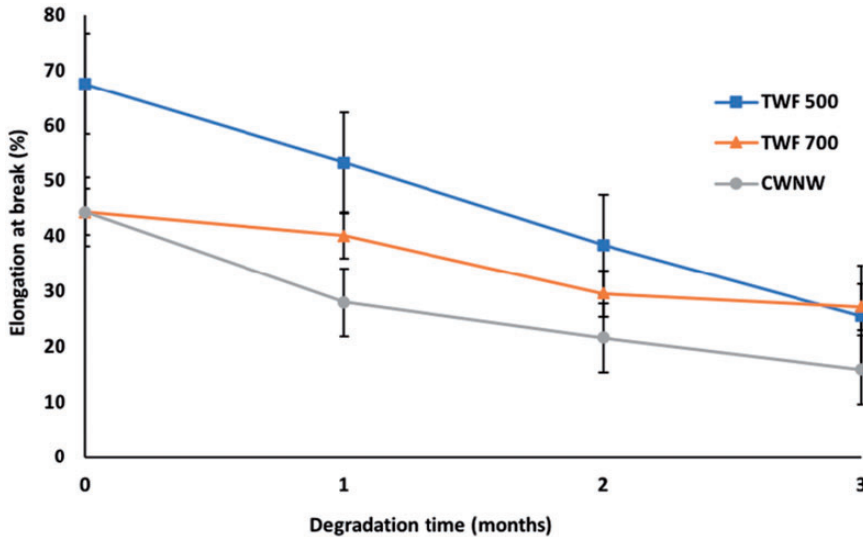
Figure 5. Elongation at break versus degradation time under accelerated weathering in the cross direction. CWNW: cotton waste nonwoven; TWF: textile waste felt.

decrease in breaking force values was continuous and linear but with lower rate after the first month. In the CD, the structure with higher density showed higher breaking force values at the beginning of the study: TWF 700 > TWF 500 > CWNW and the order did not change during the exposure time. The breaking force loss in the CD exceeded 50% after three months for the different structures. The three structures did not undergo the same decrease after exposure time showing that the composition and the type of structure have some influence on the resistance to accelerated weathering. In addition to the breaking force, the results shown in Figures 4 and 5 revealed that the exposure to accelerated weathering conditions decreased the elongation at break values in both directions which was in accordance with the work of Briassoulis et al. [38] and Spiridon et al. [39]. The decrease in elongation at break values after three months of exposure was higher in the MD than in the CD, and the loss of elongation values was higher for the structures with lower density which showed less resistance to degradation since the penetration of UV light and moisture through the structure was faster [32]: CWNW (64.27%) > TWF 500(62.2%) > TWF 700 (38.77%). In the CD, the elongation at break variation during the exposure time was lower than the variation in the MD for the different structures. The curves showed a slower decrease rate (37% for TWF 700, 18% for TWF 500 g/m^2, and 7.5% for CWNW) after three months of exposure. The elongation at break curve of TWF 500 decreased during the first month and then stabilized contrary to the elongation at break values corresponding to TWF 700 which showed more resistance at the beginning of the weathering and during the first two months before starting to decrease.
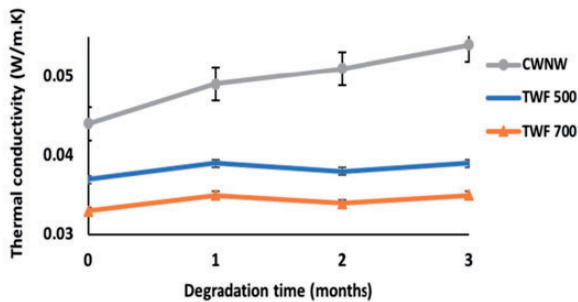
Figure 6. Thermal conductivity versus degradation time under accelerated weathering. CWNW: cotton waste nonwoven; TWF: textile waste felt.

The decrease in elongation at break values of CWNW was very low and the curve seemed stable.

Thermal conductivity and air permeability

The variation of thermal conductivity of the three samples under the effect of artificial weathering conditions was studied during three months of exposure time, and the results are shown in Figure 6.

The three samples showed an increase in thermal conductivity after three months of exposure under artificial aging conditions. The thermal conductivity increased with the decrease in density [40]. The degradation of fibers under the UV, moisture, and heat conditions makes the needle-punched nonwovens more porous and then less insulating which explains the increase in thermal conductivity values. These values were higher for natural fibers based structure CWNW comparing to blend fibers based structure TWF 500 and TWF 700 since the degradation rate of natural fibers is higher than that of synthetic ones [31].

The heating of soil is required. The TWFs, TWF 500 and TWF 700, showed more stability in thermal conductivity after three months of exposure under aging conditions which is required for mulching application.

The modification of the structure of our three samples under the effect of accelerated weathering was checked through the variation of air permeability. The results shown in Figure 7 revealed that after three months of exposure to artificial aging, the air permeability of all the samples increased. The degradation of the fibers under the effect of moisture, heat, and temperature increased the porosity of the samples and then their permeability to air [41].

The increasing of air permeability was higher for CWNW since it showed more degradation after three months of study due to its compositions based on natural fibers.

Thermal conductivity of the mulching is a factor of a primer importance that has a direct impact on the heat and solar energy transfer through the interfaces air–mulch and mulch–soil.
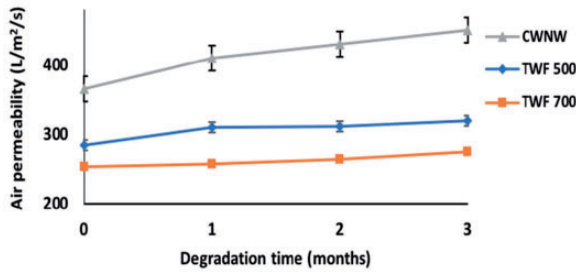
Figure 7. Air permeability versus degradation time under accelerated weathering. CWNW: cotton waste nonwoven; TWF: textile waste felt.

Table 3. Chemical composition of TWF before and after the QUV degradation.

Degradation time (months)	Moisture (%)	Non-fibrous materials (%)	Protein fibers (%)	Cellulosic fibers (%)	PET (%)	Other synthetic fibers (%)
0	1.5 ± 0.07	1.1 ± 0.05	17.6 ± 0.81	25.5 ± 1.25	51.8 ± 2.59	2.3 ± 0.3
1	1.1 ± 0.03	1.2 ± 0.06	12.4 ± 0.72	21.4 ± 1.05	61.1 ± 3.4	1.9 ± 0.08
2	1.4 ± 0.02	1.6 ± 0.08	12.3 ± 0.51	21.1 ± 2.3	61.2 ± 3.06	2.2 ± 0.5
3	1.3 ± 0.05	1.7 ± 0.08	9.4 ± 0.45	18.4 ± 0.92	67.1 ± 3.35	2.1 ± 0.11

PET: polyethylene terephthalate.

In fact, the mulch prevents evaporation [42] and enhances the amount of heat stored in or released from the upper layer of the soil [43]. Yonghui Yang et al. proved that mulching reduced water evaporation and increased crop productivity [44].

Fibrous composition variation

The TWF are blend structures obtained from textile clothing wastes and contain different types of fibers. In this work, the variation of the TWF composition exposed to accelerated weathering conditions according to the different rates of degradation of each kind of fiber during the exposure time was studied. For the reproducibility of the results, the quantitative study was repeated three times, and the results are collected in Table 3.

The variation of the fibrous composition of blended TWF is caused by the degradation of fibers with different rates during the exposure time to accelerated weathering conditions. This showed that natural fibers were significantly deteriorated. More than 45% of protein fibers and 25% of cellulosic fibers were degraded under three months of accelerated weathering condition (UV light, moisture, and heat). Synthetic fibers were less subjected to the degradation process.

After three months of exposure, the amount of both natural and synthetic fibers is decreasing with a higher rate for the natural ones. As a consequence, the percentage of synthetic fibers in the tested sample was higher compared to the percentage of natural fibers.

Between the first and the second month, the composition is almost the same and the percentage of different fibers is almost unchanged. This same aspect of plateau was observed in the weight loss study of TWF 500 and TWF 700 which confirmed the previous results regarding the slow degradation rate under accelerated weathering conditions related to this period [35].

Differential scanning calorimetry

The influence of the accelerated weathering conditions of UV light, humidity, and heat on the thermal parameters of textile waste structures were revealed by the DSC. The T_g (glass transition temperature), T_c (crystallization temperature), T_m (melting temperature), and T_d (decomposition temperature) and the corresponding enthalpies ΔH_c (crystallization enthalpy), ΔH_m (melting temperature), and ΔH_d (decomposing enthalpy) were followed during three months of exposure time. Results are shown in Table 4. For both structures, the DSC thermograms showed an endothermic peak under 100°C corresponding to the water desorption. The peak intensity is proportional to the amount of water present in the samples. The endotherm corresponding to the glass transition temperature could be overshadowed by the endotherm resulting from the moisture removal [45]. The simulated weathering conditions induced a decrease in T_g for the TWF during the

Table 4. Effect of accelerated weathering conditions on the thermal parameters of textile waste nonwoven as determined by differential scanning calorimetry.

Sample	Weathering time (months)	T_g (°C)	T_c (°C)	ΔH_c (J/g)	T_m (°C)	ΔH_m (J/g)
TWF	0	81 ± 4.05	252 ± 1.5	13.1 ± 0.7	319 ± 3.5	630.1 ± 7.4
	1	79 ± 3.9	251 ± 1.2	8.5 ± 0.4	314 ± 2.9	526.1 ± 11.6
	2	66 ± 3.2	250 ± 0.5	4.5 ± 0.1	314 ± 3.8	482.7 ± 6.9
	3	64 ± 2.8	251 ± 0.7	5.1 ± 0.2	311 ± 1.4	162.7 ± 10.2

Sample	Weathering time (months)	T_{dehy} (°C)	T_d (°C)	ΔH_d (J/g)
CWNW	0	78 ± 2.6	358 ± 3.4	121.8 ± 5.3
	1	70 ± 1.8	356 ± 2.8	90.7 ± 3.8
	2	68 ± 2.2	353 ± 3.1	89.2 ± 4.1
	3	66 ± 0.9	342 ± 2.9	69.4 ± 2.8

CWNW: cotton waste nonwoven; TWF: textile waste felt.

exposure time reflecting the decrease in molecular weight and the degradation of macromolecular chains under UV, moisture and heat. The decrease in T_g for the TWF was higher after the first month indicating that the accelerated weathering enhanced the degradation and resulted in a structural reorganization during the exposure time [37]. The melting temperature T_m also decreased during the artificial weathering as well as the corresponding enthalpy which lost 74% of its value after three months. This could be explained by the weakening of the structure which required less energy to melt since it was already degraded [39]. The same trend was observed for the CWNW thermal parameters. The decomposition temperature decreased with the incremental weathering time as well as the corresponding enthalpy which lost 43% of its value before accelerated weathering.

The DSC thermograms of the TWF showed in Figure 8 revealed different endothermic and exothermic peaks corresponding to the modification of the structure or the degradation of different fibers present in the blended structure. At 250°C, an endotherm related to the degradation of polyester. Another exothermic peak between 300°C and 320°C corresponding to the melting point of the sample is mainly composed by polyester followed by a decomposition peak at 350°C [46]. A last endothermic peak at 70°C corresponding to the decomposition of cellulose, cotton fibers present in the blended structure [47]. Some unidentified peaks with different intensities were observed and could be related to textile dyes [48] or chemical treatments residues [49] present in the textile waste structure. Regarding the
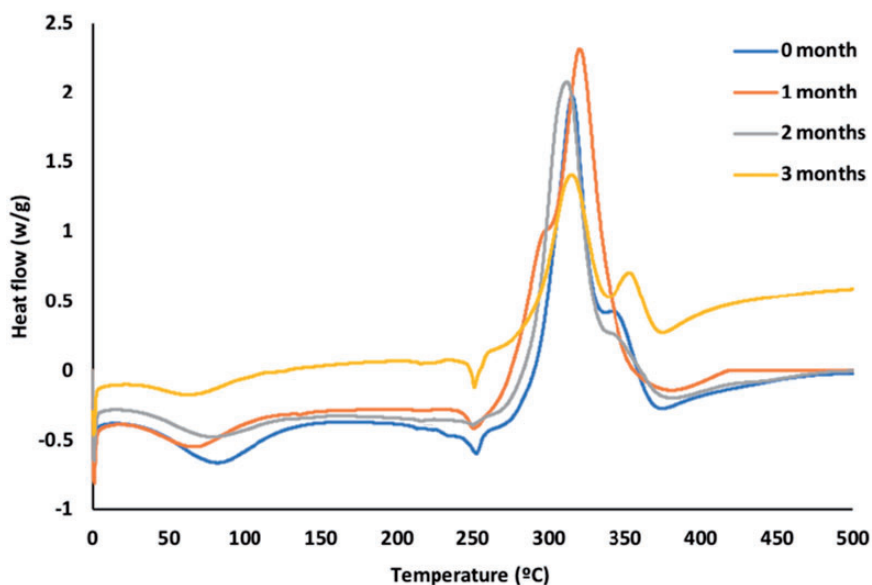

Figure 8. Effect of exposure time to accelerated weathering on the thermal parameters of the TWF revealed by DSC thermograms.
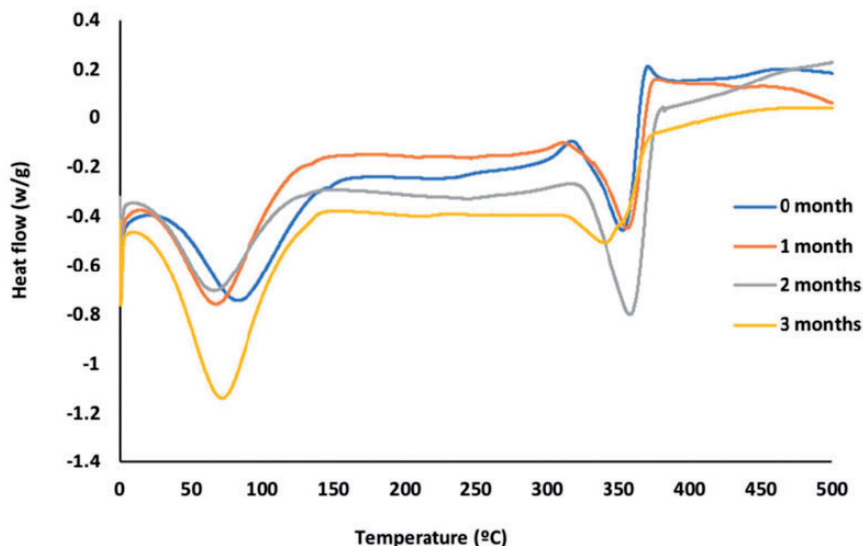
Figure 9. Effect of exposure time to accelerated weathering on the thermal parameters of the CWNW revealed by DSC thermograms.

CWNW, the decomposition temperature T_d of the cellulosic fibers and the corresponding enthalpy ΔH_d underwent a similar variation to the thermal parameters of TWF and decreased with the incremental exposure time. The accelerated weathering conditions enhanced the chains scission and degraded the fibers and the resulting weathered samples became more brittle and required less energy to decompose [39]. The CWNW DSC thermograms in Figure 9 showed an endothermic peak at 360°C related to the heat absorption due to the decomposition of cellulose [50]. A small peak was also observed between 430°C and 450°C and could be attributed to the final stage of degradation of the cotton samples [47].
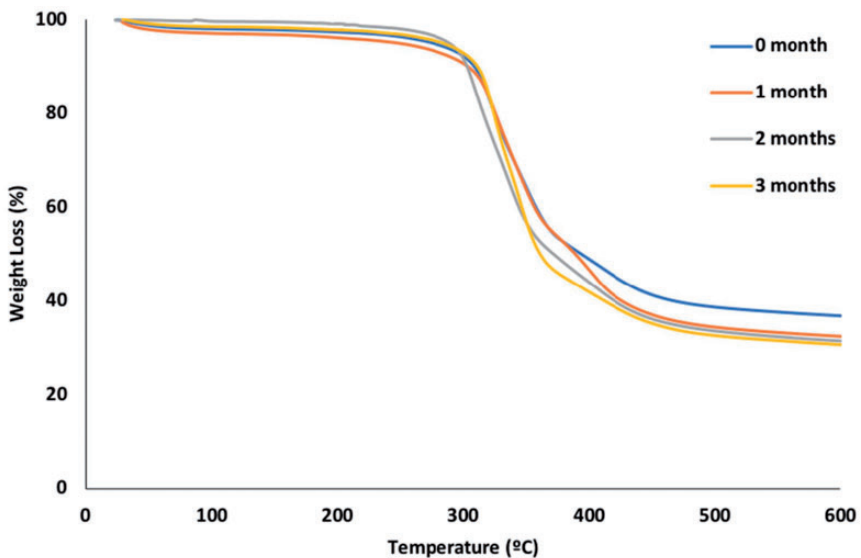
Thermogravimetric analysis

The weight loss as a function of the temperature was studied for TWF and CWNW during the exposure time under accelerated weathering conditions. The variation of thermal parameters before and after artificial weathering of samples was reported in Table 5. T_{onset} is the initial degradation temperature, T_{endset} is the complete degradation temperature, W% (weight loss percentage), and final residue (final residue percentage at the end of degradation) were followed during the study. The TGA and derivative thermogravimetric (DTG) curves are shown in Figures 10 to 13.

The accelerated weathering conditions enhanced the thermal degradation of the different structures. The exposure to UV light, moisture, and heat decreased the thermal stability of TWF and CWNW. The more the samples are weathered,

Table 5. Effect of accelerated weathering conditions on the thermal parameters of textile waste non-woven as determined by thermogravimetric analysis.

Sample	Weathering time (months)	T_{onset} (°C)	T_{peak} (°C)		T_{endset} (°C)	W%	FR%
TWF	0	276 ± 4.3	317 ± 2.3	356 ± 4.5	490 ± 5.6	56 ± 2.3	37 ± 1.3
	1	267 ± 4.8	327 ± 1.7	343 ± 3.2	474 ± 4.8	58.6 ± 2.1	32.4 ± 0.9
	2	214 ± 2.5	314 ± 2.8	335 ± 5.7	467 ± 4.3	63.9 ± 2.4	31.4 ± 2.1
	3	203 ± 3.2	322 ± 3.1	346 ± 2.7	456 ± 3.6	63.1 ± 1.9	30.6 ± 0.9
CWNW	0	267 ± 3.5	342 ± 5.5		473 ± 3.7	68.7 ± 2.2	20.5 ± 0.5
	1	237 ± 5.1	355 ± 4.3		459 ± 4.2	77.4 ± 0.8	14.2 ± 1.3
	2	232 ± 4.1	354 ± 3.2		443 ± 2.8	85.1 ± 0.9	5.2 ± 0.9
	3	218 ± 3.7	344 ± 2.8		435 ± 2.9	93.7 ± 1.2	0.1 ± 0.06

CWNW: cotton waste nonwoven; FR: final residue; TWF: textile waste felt.

Figure 10. Effect of exposure time to accelerated weathering on the thermogravimetric analysis for TWF.

the higher is the degradation rate [51]. The thermogravimetric curves showed a multi-step decomposition for both samples. The thermal degradation for CWNW exposed to simulated weathering conditions is higher than TWF since the latter contains less natural fibers which degrade faster than synthetic ones [31]. The weight loss increased with the exposure time for TWF and CWNW. After three
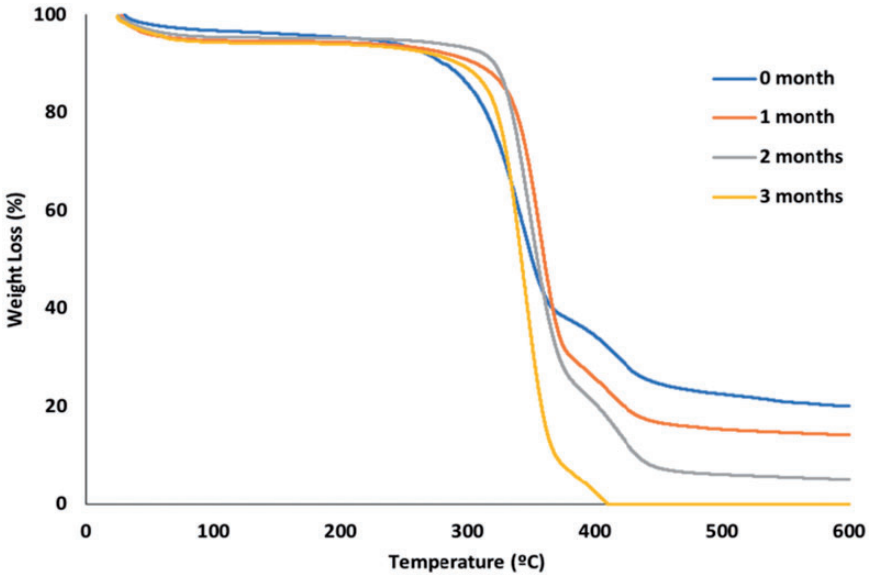
Figure 11. Effect of exposure time to accelerated weathering on the thermogravimetric analysis for CWNW.
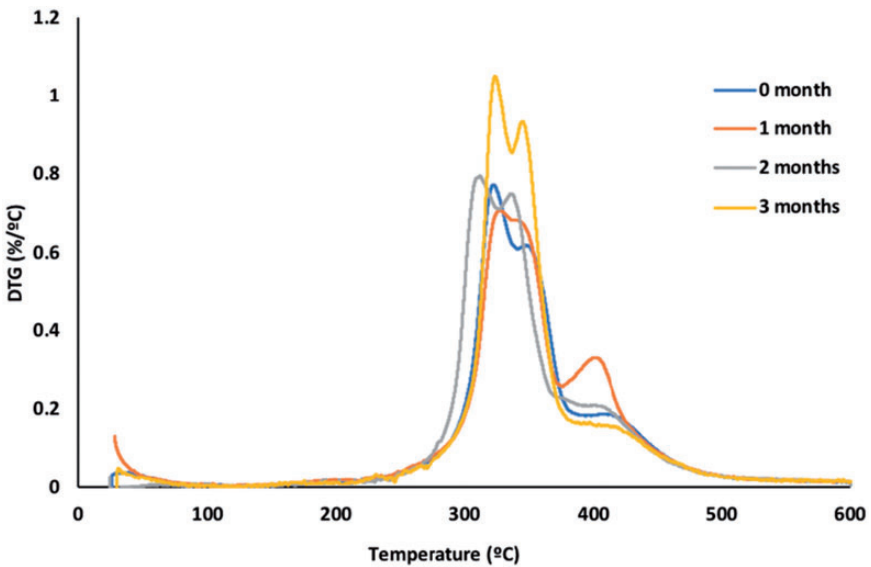

Figure 12. Effect of exposure time to accelerated weathering on the differential thermogravimetric (DTG) curves for TWF. DTG: derivative thermogravimetric.
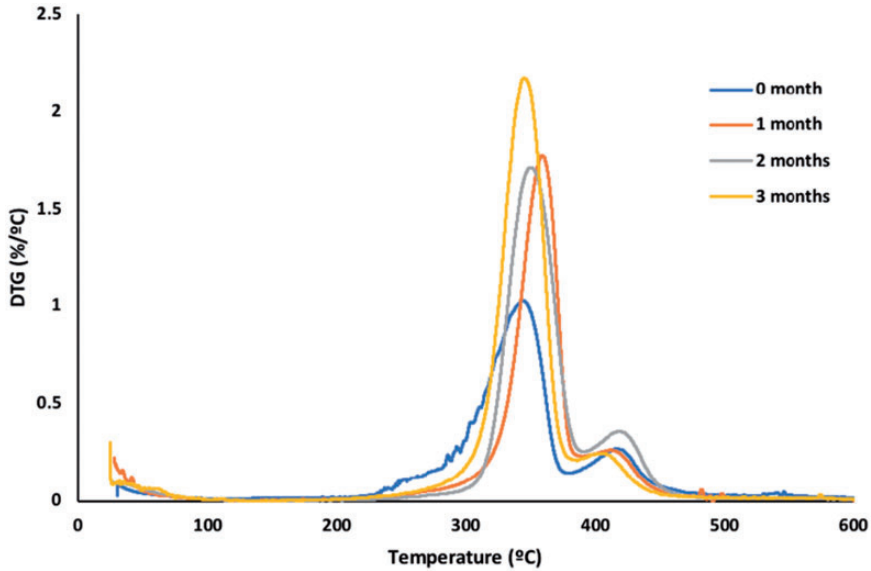
Figure 13. Effect of exposure time to accelerated weathering on the differential thermogravimetric (DTG) curves for CWNW. DTG: derivative thermogravimetric.

months, the CWNW was completely decomposed at 410°C as shown in Figure 11 contrary to TWF which showed more resistance to artificial weathering, and the final residue was more than 30% at 600°C after the same exposure time as shown in Figure 10. The DTG curves shown in Figures 12 and 13 revealed that the degradation process temperatures T_{onset} and T_{endset} decreased with the exposure time for both structures. The combined action of UV light, moisture, and heat embrittled the structures and then enhanced its thermal degradation [52], and the starting temperatures of thermal degradation are lower for weathered samples. The DTG curves for TWF in Figure 12 showed two maximum degradation peaks contrary to CWNW in Figure 13 with only one maximum peak and this could be explained by the presence of different fibers in the blended structure of the former. The small peak in the DTG curves around 400°C confirmed the multi-step degradation for both samples already revealed by TGA curves. The temperatures corresponding to the maximum degradation alternated between increasing and decreasing. The decrease could be due to the reduction of molecular weight of samples constituents and the increase could be related to the increase in the thermal stability of the samples due to the crystallinity enhancement or the formation of cross links after the degradation of amorphous components [53].

Dynamic mechanical analysis

The effect of accelerated weathering conditions (UV light, humidity, and heat) on the dynamic mechanical properties of the different samples was studied. The DMA

Table 6. Effect of accelerated weathering conditions on the thermal parameters of textile waste nonwoven as determined by dynamic mechanical analysis.

Sample	Weathering time (months)	T_g (°C)	E'_{25} (MPa)	E'_{75} (MPa)	E'_{125} (MPa)
TWF	0	118 ± 3.2	20.1 ± 1.4	17.4 ± 0.5	12.8 ± 1.1
	1	114 ± 2.7	18.9 ± 2.6	15.3 ± 1.8	9.6 ± 1.4
	2	107 ± 3.7	13.5 ± 2.7	9.8 ± 1.2	4.1 ± 0.6
	3	106 ± 2.2	10.8 ± 1.9	8.3 ± 0.9	4 ± 0.6
CWNW	0	–	755.1 ± 4.3	610.7 ± 7.2	419.2 ± 5.3
	1		307.8 ± 3.6	309.3 ± 7.6	273.9 ± 8.4
	2		20.7 ± 1.9	18.64 ± 3.4	15.1 ± 2.4
	3		7.9 ± 0.8	8.07 ± 1.9	7.1 ± 1.2

CWNW: cotton waste nonwoven; TWF: textile waste felt.

data were used to determine the values of storage modulus E' at different temperatures as well as the glass transition temperature T_g defined as the temperature corresponding to the maximum of the damping factor Tan δ. The variation of storage modulus E' and the glass transition temperature T_g were followed during three months of exposure. The effect of exposure time on these parameters was reported in Table 6. The DMA data revealed that the UV radiation, moisture vapor, and heat effect decreased the mechanical properties of CWNW and TWF with a higher rate for the former [54]. During the accelerated weathering, the repeated cycles altering UV light and moisture under high temperature degraded the fibers and decreased the mechanical performances of the samples. The absorption of moisture due to the water vaporization wetted the sample and caused the fibers swelling. The second half of the weathering cycle dried the sample and the moisture desorption resulted in fibers contraction. This altering swelling-contraction degraded gradually the fiber and thus the textile structure [55,56]. The cleavage of chemical bonds and the degradation of the fibrous networks under the action of UV, humidity, and heat during the exposure time in the accelerated weathering machine induced a variation in storage modulus E' and damping factor Tan δ [55]. The glass transition temperature was identified from the Tan δ curves showed in Figure 16. The T_g values of weathered TWF decreased with incremental degradation time because of the chain scission of polymers due to photochemical degradation. The combined actions of UV light, moisture, and heat decreased the molecular weight of the polymers and then decreased the glass transition temperature of TWF [56]. The storage modulus E' of the weathered TWF samples shown in Figure 14 and the cellulosic fibers presents in CWNW shown in Figure 15 decreased with exposure time. It tumbled down considerably after two months of artificial weathering and lost 97% comparing to its initial value before weathering. for the CWNW samples. The degradation rate of E' for TWF samples was
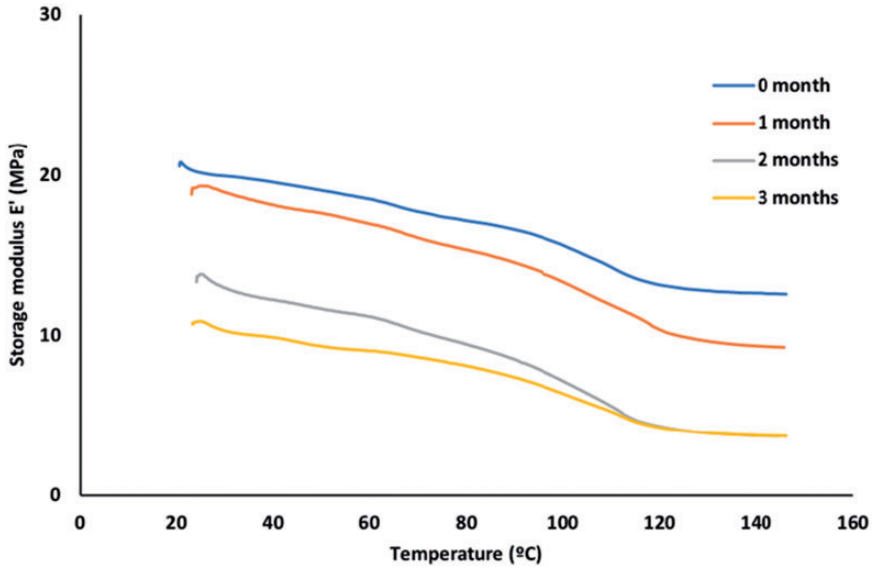
Figure 14. Effect of exposure time to accelerated weathering conditions on storage modulus E' for TWF.
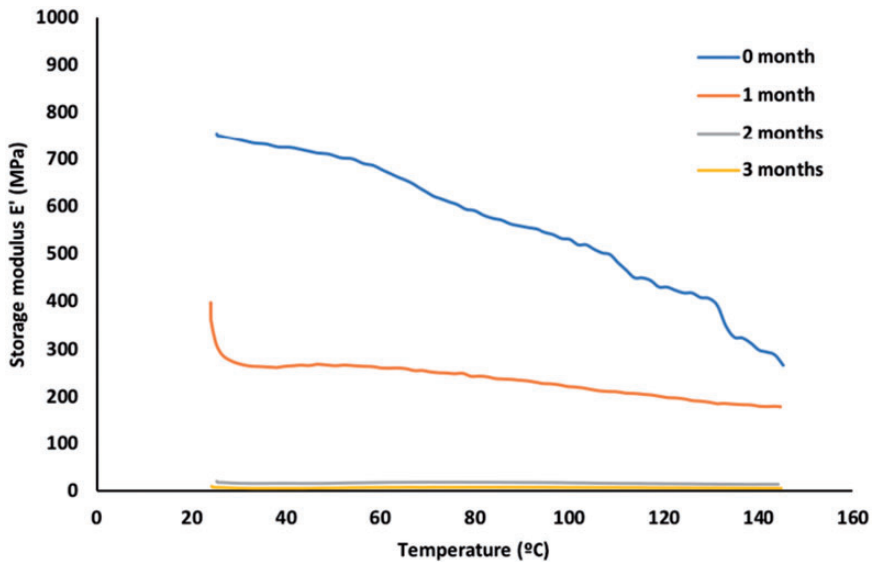

Figure 15. Effect of exposure time to accelerated weathering conditions on storage modulus E' for CWNW.
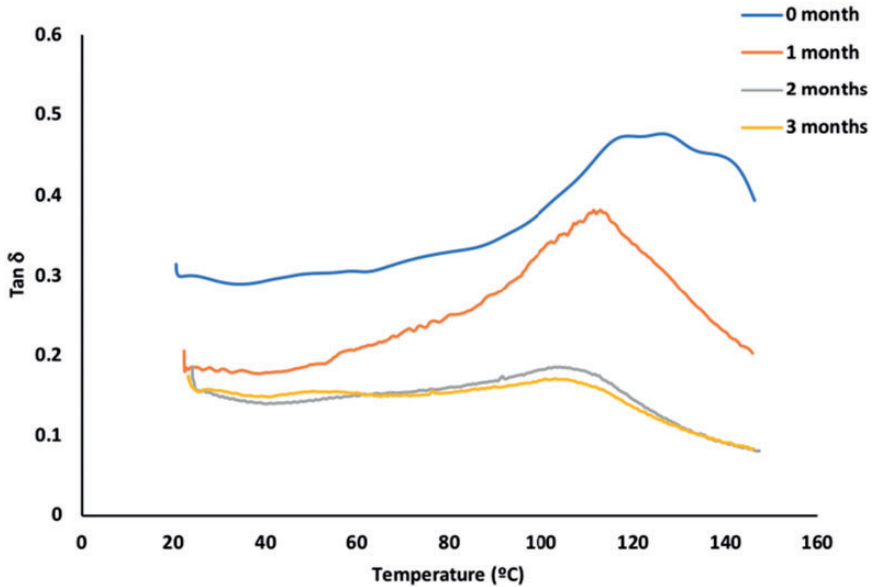
Figure 16. Effect of exposure time to accelerated weathering conditions on Tan δ for TWF.

lower than weathered CWNW and loosed 53% of its value after the third month at the same range of temperature. The synthetic fibers present in TWF showed more resistance comparing to cellulosic ones in CWNW under accelerated weathering conditions, but both structures underwent a decrease in mechanical and thermal properties under the effect of UV, moisture, and heat [57]. The glass transition temperature was identified from the Tan d curves shown in Figure 16. The Tg values of weathered TWF decreased with incremental degradation time because of the chain scission of polymers due to photochemical degradation. The combined actions of UV light, moisture, and heat decreased the molecular weight of the polymers and then decreased the glass transition temperature of TWF [56].

Analysis of statistical significance

To decide if there is a significant difference between compared values, student statistical test is used. In student test commonly called T test, a standardized value calculated from samples data during a hypothesis test used to determine whether to reject the null hypothesis. When hypothesis tests compare two experimental samples data under the null hypothesis, the comparison is based on the test statistic. Values of a test statistic correspond to p values for the hypothesis test. Therefore, when the data present strong evidence against the assumptions in the null hypothesis, the magnitude of the test statistic becomes large and the test's p value may become small enough to reject the null hypothesis.

Table 7. Monthly variation of p values.

		TWF 500			TWF 700			CWNW			
		0/1	1/2	2/3	0/1	1/2	2/3	0/1	1/2	2/3	
Weight loss		0.83	0.955	0.613	0.373	0.865	0.633	0.581	0.868	0.829	
Tensile properties	Breaking force MD	0.03	0.01	0.001	0.003	0.002	0.001	0.001	0.004	0.001	
	Breaking force CD	0	0	0.006	0	0.001	0.008	0	0.001	0.005	
	Elongation at break CD	0	0.008	0.001	0.003	0.002	0.108	0.002	0.003	0.002	
	Elongation at break MD	0.003	0.884	0.707	0.559	0.568	0.001	0.931	0.37	0.542	
Thermal conductivity		0.182	0.288	0.603	0.07	0.288	0.232	0.004	0.07	0.031	
Air permeability		0	0.087	0.003	0.014	0.009	0.001	0	0	0	
Quantitative fibrous composition	Protein fibers	0.007	0.758	0.014							
	Cellulosic fibers	0.013	0.709	0.007							
	PET	0.004	0.792	0.002							
DSC	T_g (°C) [CWNW: T_{dehy} (°C)]	0.302	0.006	0.359				0.014	0.302	0.302	
	T_c (°C) [CWNW: T_d (°C)]	0.747	0.765	0.911				0.595	0.465	0.206	
	ΔH_c (J/g) [CWNW: ΔH_d (J/g)]	0.002	0.001	0.129				0	0.368	0.001	
	T_m (°C)	0.127	1	0.274							
	ΔH_m (J/g)	0	0.002	0							
TGA	T_{onset} (°C)	0.04	0	0.013				0.001	0.128	0.005	
	T_{peak} (°C)	0.063	0.052	0.154				0.015	0.689	0.025	
	T_{endset} (°C)	0.006	0.04	0.016				0.012	0.008	0.144	
	W%	0.063	0.016	0.491				0.018	0.014	0.005	
	FR%	0.088	0.565	0.231				0.008	0	0.002	
DMA	T_g (°C)	0.041	0.002	0.038							
	E'_{25} (MPa)	0.005	0	0.004				0	0	0	
	E'_{75} (MPa)	0.022	0	0.001				0	0	0	
	E'_{125} (MPa)	0	0	0.028				0	0	0	

CWNW: cotton waste nonwoven; FR: final residue; TWF: textile waste felt; MD: machine direction; CD: cross direction; DSC: differential scanning calorimetry; TGA: thermogravimetric analysis; DMA: dynamic mechanical analysis; PET: polyethylene terephthalate.

T test uses the t statistic. Suppose one conduct a two-tailed t test with an α level of 0.05 and obtain a p value of 0.040. Because this p value is less than ones chosen α level, one declares statistical significance, rejects the null hypothesis, and then we can conclude that the two samples are different.

For each characterization parameter, three measurements were done and compared using MINITAB Software. The results of p value's monthly variation (0 month/1 month, 1 month/2 months, and 2 months/three months) are in following table:

The p values corresponding to the different mechanical characterization (breaking force in both directions, dynamic mechanical values) were lower than 0.05 which means that there is a significant difference related to the degradation of the three structures under the effect of accelerated aging conditions. The aging test weakened the textile structures without an obvious deterioration of the fiber giving the unchanged weight loss.

Regarding the thermal conductivity, the p values were higher than the chosen α level which means that there is no significant difference since the aging tests did not induce a deterioration of the TWF structures contrary to the CWNW which showed a significant difference due to the higher degradation rate of natural fibers comparing to synthetic ones. The thermal properties showed a considerable variation under the effect of accelerated weathering conditions, and the p values of the majority of thermal parameters were less than 0.05 which corresponds to a significant difference. The values exceeding 0.05 could be explained by an unchanged value like the crystallization temperature T_c which stayed unchanged after three months of test as well as the decomposition temperature T_d.

FTIR spectroscopy

The effect of accelerated weathering conditions on the chemical structure of the samples was studied. The chemical changes of textile structures under UV light, moisture, and heat was followed during the exposure time. The FTIR spectroscopy was used to investigate the variation of functional groups of the weathered samples during the exposure time. The functional groups corresponding to the peaks wavenumbers in FTIR spectra during all the weathering period are reported in Table 8.

FTIR spectra before and after accelerated weathering are given in Figures 17 to 20. The FTIR spectra showed that the accelerated weathering caused mainly changes in the absorption intensities at different bands for both structures. These variations are related to changes in chemical composition of the functional groups of the tested samples because of the combined effect of UV light, moisture, and heat. For CWNW, the simulated weathering conditions decreased the peak intensity of O–H stretching band at $3332 \, cm^{-1}$ and C–H stretching band at $2900 \, cm^{-1}$. This decrease is due to rupture of hydrogen bonds, methyl, and methylene groups of cellulose [31] under the effect of UV light, moisture, and heat. The consequence of accelerated weathering was also the shift of bands wavenumbers. The band at $1635 \, cm^{-1}$ from the H–O–H bending of the absorbed water was shifted to

Table 8. Peaks assignment for absorbed infrared radiations from FTIR spectra of TWF and CWNW before and after accelerated weathering [53].

CWNW		TWF	
Wavenumber (cm^{-1})	Corresponding Functional group	Wavenumber (cm^{-1})	Corresponding functional group
3332	O–H stretching	3741	O–H stretching (cellulose)
2893	C–H stretching	3278	N–H stretching (wool)
1635	H–O–H bending of absorbed water	2916	C–H stretching (PET)
1427	Symmetric C–H bending	2237	Nitrile C=N stretch (acrylic)
1311	C–C and C–O skeletal vibrations	1712	C=O of ester carbonyl group (PET)
1242	O–H in plane bending	1651	C=O elastic vibration (wool)
1157	C–O–C asymmetrical stretching	1519	C–N–H bending deformation (wool)
1103	asymmetric glucose ring stretching	1465	CH$_3$ bend (PET)
1056	C–O stretching	1365	C–H deformation (PET)
1026	C–C stretching	1234	C–O stretching (PET)
–	–	1157	C–O–C asymmetrical stretching (cellulose)
–	–	1049	C–O stretching (cellulose)
–	–	1026	C–C stretching (cellulose)
–	–	817	C–C stretching (PET)

CWNW: cotton waste nonwoven; TWF: textile waste felt; PET: polyethylene terephthalate.

1643 cm^{-1}, and the band of O–H bending at 1242 cm^{-1} was shifted to 1265 cm^{-1}. The bands at 1056 cm^{-1} indicating C–O stretching at C3 and C–O stretching at C6 was shifted to 1049 cm^{-1} and gave a slight shoulder at 1157 cm^{-1} which corresponds to asymmetric bridge stretching of C–O–C groups in cellulose and hemicellulose [31]. The symmetric C–H bending at 1427 cm^{-1} and the band at 1311 cm^{-1} for C–C and C–O skeletal vibrations peaks showed an increase in peak intensity after exposure under accelerated weathering conditions but without band shift. The peak intensity of C–C stretch band at 1026 cm^{-1} stayed unchanged and kept the same wavenumber during all the exposure time showing a high resistance to degradation despite the accelerated weathering conditions. The presence of a peak at 1712 cm^{-1} could be related to presence of ester carbonyl group present in polyester yarns used along the MD to reinforce the cotton nonwoven. Regarding TWF, the FTIR spectra showed more peaks because of the presence of different fibers in this blended structure such as cotton, wool, acrylic, and mainly polyester. The accelerated weathering decreased the intensity of the different IR bands between 4000 cm^{-1} and 700 cm^{-1} due to the
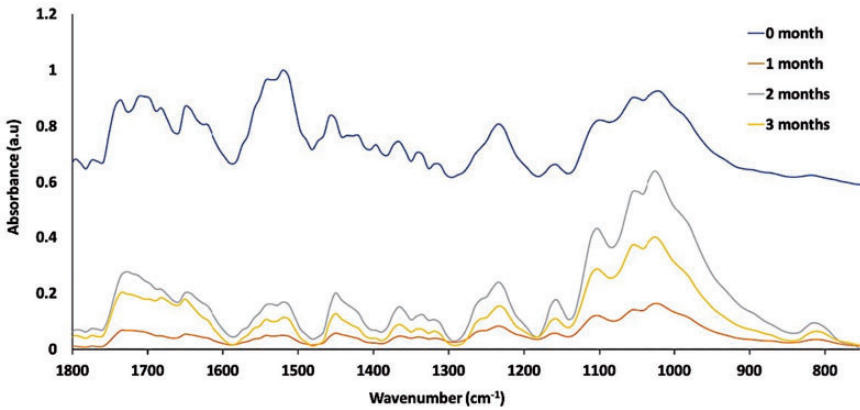
Figure 17. FTIR spectra for TWF before and after accelerated weathering (800 cm^{-1}–1800 cm^{-1}).
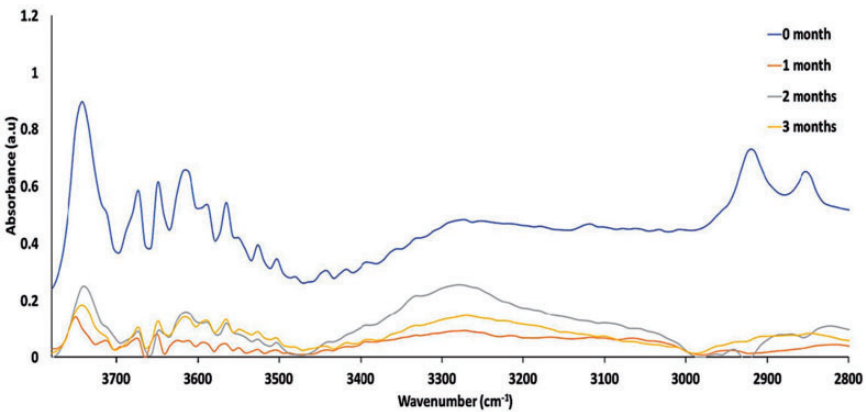

Figure 18. FTIR spectra for TWF before and after accelerated weathering (2800 cm^{-1}–3700 cm^{-1}).

photolysis and hydrolysis actions by UV light, moisture vapor, and heat leading to a random main chains scission [58]: the C–C stretching band at 817 cm^{-1}, the C–O stretching peaks at 1234 and 1049 cm^{-1}, the C–H deformation peaks at 1365 cm^{-1}, the C–O stretching peaks at 1049 cm^{-1} for cellulosic fibers; the C–N–H bend at 1519 cm^{-1} and the C=O elastic vibration at 1651 cm^{-1} for wool fibers; the C=N stretch at 2237 cm^{-1} for acrylic fibers; and the C–H stretching band at 2916 cm^{-1} for polyester fibers. The decrease in the peaks absorbance intensity showed the modification of the structure of TWF. Its surface became more brittle under the accelerated weathering conditions because of crosslinking caused by the recombination of generated free radicals resulting from the Norrish reaction type I under the UV light effect [59]. The CH$_3$ band (polyester) at 1465 cm^{-1} was shifted to 1450 cm^{-1} as well as
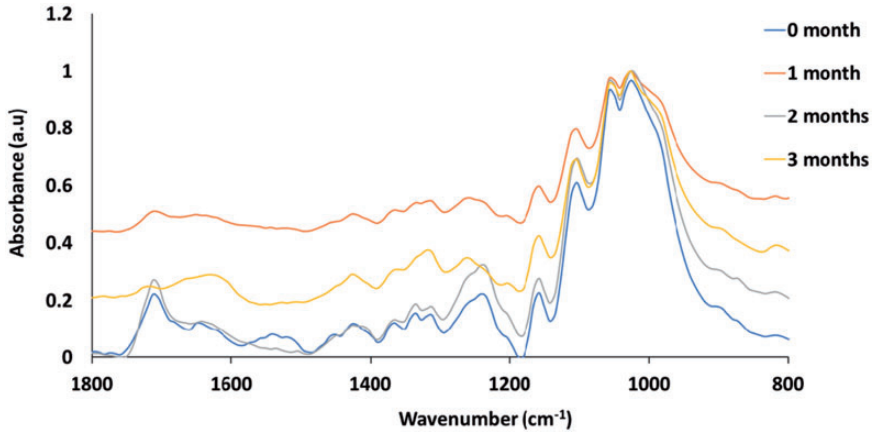
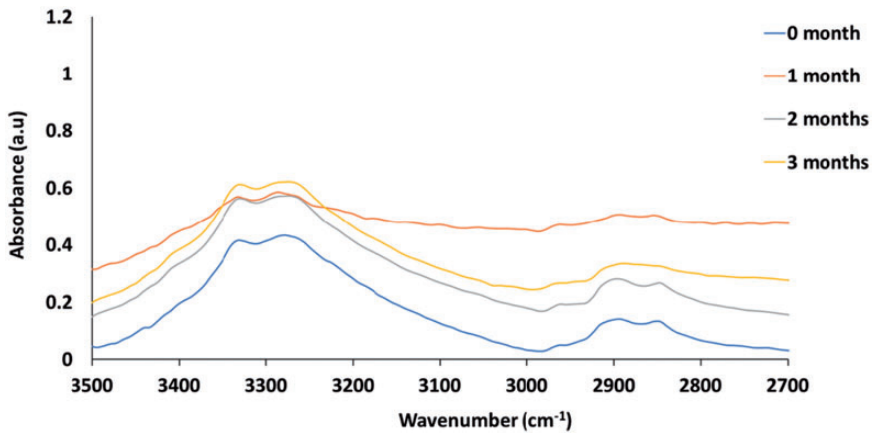**Figure 19.** FTIR spectra for CWNW before and after accelerated weathering (800 cm^{-1}–1800 cm^{-1}).

Figure 20. FTIR spectra for CWNW before and after accelerated weathering (2700 cm^{-1}–3500 cm^{-1}).

the ester carbonyl group C=O band at 1712 cm^{-1} (polyester) was shifted to 1728 cm^{-1}. The intensity of the latter decreased due to the action of photo-oxidation and hydrolysis leading to the formation of carboxylic acid and ketones [58]. The C–C stretching at 1026 cm^{-1} for cellulosic fibers showed less resistance to accelerated weathering because of the textile waste origin of TWF and the different degradation that the fibers underwent before ending in a the TWF structure contrary to raw cotton fibers in CWNW. Above 3000 cm^{-1}, N–H stretching band (wool) at 3278 cm^{-1} showed a decrease as well as O–H stretching band at 3741cm^{-1} due to the forming of new free OH groups after exposure under accelerated weathering

conditions [53]. The variation of some peaks could not be followed since they are not repeatable during all the study and appeared or disappeared at spectra done after each month of the weathering study. This could be explained by the random disposition of the fibers in the blended TWF structure which make one peak appear for one sample but not for another one and the variation of the peak's intensity or the shift of wavenumber is not necessary related to accelerated weathering conditions. It could be also explained by the depth of penetration of UV light and the propagation of photodegradation along the sample which change with the change of structure composition and its components disposition [59].

Conclusions

The effect of accelerated weathering conditions on the mechanical, thermal, and physicochemical properties of clothing textile waste and cotton spinning waste nonwovens was investigated. The evolution of these properties was studied during three months of exposure in a QUV machine. The objective of the study was to understand the mechanism of degradation of TWF and CWNW under the effect of UV light, moisture, and heat. The results showed that the accelerated weathering of mulching structures decreased their weight as well as their mechanical properties. The three samples showed a decrease in breaking force and elongation at break during all the exposure time. The fibrous composition variation of the blended TWF structure gave an idea about the degradation of both natural and synthetic fibers under accelerated weathering and confirmed the faster rate for natural ones. The thermal parameters revealed by DSC analysis and TGA results showed that the accelerated weathering conditions enhanced the thermal degradation of both structures. The exposure under UV light, moisture, and heat decreased the thermal stability of TWF 500, TWF 700, and CWNW, and the degradation rate is higher for the more weathered samples. The mechanical properties revealed by DMA also decreased, and the structures are more brittle, and their mechanical resistance is lower after accelerated weathering. The effect of accelerated weathering conditions on the structure of both TWF and CWNW and the chemical changes of functional groups was also investigated via FTIR spectroscopy. The FTIR spectra showed that intensity peaks of IR bands decreased due to the photolysis and hydrolysis actions by UV light, moisture vapor, and heat leading to a random main chain scission. The spectra also showed the disappearance of some functional groups and the generation of new radical groups resulting from Norrish reaction type I leading to crosslinking and intensities variations.

   Overall, the mulching mats based on textile wastes used during this study showed a good resistance to the accelerated weathering conditions and their degradation was not significant which makes them a promising sustainable alternative for plastic films used currently. Furthermore, their thick layer might combine soil moisture retention with excellent soil warming properties. This can be confirmed by a further study of the tested structures in agricultural field and their effect on properties of plants and soil.

ORCID iD

Houcine Abidi ⓘ https://orcid.org/0000-0002-8541-6296

References

[1] Pritchard M, Sarsby RW and Anand SC. *Handbook of technical textiles*. Bolton, UK: Department of the Built Environment, Faculty of Technology, Bolton Institute, 2000. DOI: 10.1533/9781855738966.372.

[2] Palamutcu S and Devrent N. Technical textiles for agricultural applications. *Int interdis J sci res* 2017; 3: 1–8.

[3] Fisher G. *Agrotextiles: A growing landscape with huge potential*. Textile Media Services Ltd, 2013.

[4] Agrawal SK. Application of textile in agriculture. *IJARSE* 2013; 8354: 9–18.

[5] Credence Research. *Agro textile market by product type (shade net, mulch mat, ground cover, crop cover, insect net, pond liners),by application (crop production, animal husbandry, horticulture & floriculture) – growth, future prospects and competitive analysis*, 2017–2025. San Jose, CA: Credence Research.

[6] Kasirajan S and Ngouajio M. Polyethylene and biodegradable mulches for agricultural applications: a review. *Agron Sustain Dev* 2012; 32: 501–529.

[7] Sintim HY and Flury M. Is biodegradable plastic mulch the solution to agriculture's plastic problem? *Environ Sci Technol* 2017; 51: 1068–1069.

[8] He G, Wang Z, Li S, et al. Plastic mulch: tradeoffs between productivity and greenhouse gas emissions. *J Clean Prod* 2018; 172: 1311–1318.

[9] Gu X-B, Li Y-N and Du Y-D. Biodegradable film mulching improves soil temperature, moisture and seed yield of winter oilseed rape (*Brassica napus* L.). *Soil Tillage Res* 2017; 171: 42–50.

[10] Paul P, Sanyal P and Gon D. Application of natural fibres in agrotextiles. *Indian Text J*, www.indiantextilejournal.com/articles/FAdetails.asp?id = 4709 (2012, accessed 24 May 2019).

[11] Zhang H, Cookson P and Wang X. A comparative study on accelerated weathering tests of wool fabrics. *Text Res J* 2008; 78: 1004–1010.

[12] Luo J, Chen Z and Zhang KY. Preparation and characterization of biodegradable cotton mulching film. *Appl Mech Mater* 2013; 368–370: 791–794.

[13] Bhattacharyya R, Fullen MA, Davies K, et al. Utilizing palm-leaf geotextile mats to conserve loamy sand soil in the United Kingdom. *Agric Ecosyst Environ* 2009; 130: 50–58.

[14] Dinu I and Saska M. Production and properties of soil erosion control mats made from sugarcane bagasse. *Journal of American Society of Sugarcane Technologists ASSCT* 2006; 27: 36–47.

[15] Rawal A and Anandjiwala R. Comparative study between needlepunched nonwoven geotextile structures made from flax and polyester fibres. *Geotext Geomembr* 2007; 25: 61–65.

[16] Saha P, Roy D, Manna S, et al. Durability of transesterified jute geotextiles. *Geotext Geomembr* 2012; 35: 69–75.

[17] Pandey Y. Preparation and utilization of woven and nonwoven fabrics of *Girardinia diversifolia, Agave sisalana* and bagasse fibres for agro textiles. *Krishikosh Institutional Repository* 2012; 172–175. http://krishikosh.egranth.ac.in/handle/1/69407.

[18] Subaida EA, Chandrakaran S and Sankar N. Experimental investigations on tensile and pullout behaviour of woven coir geotextiles. *Geotext Geomembr* 2008; 26: 384–392.

[19] Asma T. Adhesion characterization of alfa fibres in unsaturated polyester matrix. *IJARTEX* 2014; 2: 18–29.

[20] Sunilkumar NM. Agro textiles – their applications in agriculture and scope for utilizing natural fibers in agro tech sector. *Internat J Appl Home Sci* 2017; 4: 653–662.

[21] Bhavani K, Mallikarjun N and Sunilkumar NM. Agro textiles – their applications in agriculture and scope for utilizing natural fibers in agro tech sector. *Int J Appl Home Sci* 2017; 4: 653–662.

[22] Dierickx W and Van Den Berghe P. Natural weathering of textiles used in agricultural applications. *Geotext Geomembr* 2004; 22: 255–272.

[23] Gibbs D. Durability of polyester geotextiles subjected to australian outdoor and accelerated weathering durability of polyester geotextiles subjected to australian outdoor. In: *International Congress on Environmental Geotechnics*, Melbourne, Australia, November 2014.

[24] Gulmine JV, Janissek PR, Heise HM, et al. Degradation profile of polyethylene after artificial accelerated weathering. *Polym Degrad Stab* 2003; 79: 385–397.

[25] Carvalho R and Fangueiro R and Neves J. Durability of natural fibers for geotechnical engineering. *Key Eng Mater* 2014; 634: 447–454.

[26] Milošević M, Krkobabić A, Radoičić M, et al. Biodegradation of cotton and cotton/polyester fabrics impregnated with Ag/TiO$_2$ nanoparticles in soil. *Carbohydr Polym* 2017; 158: 77–84.

[27] Ferrándiz M, Capablanca L, García D, et al. Application of antimicrobial microcapsules on agrotextiles. *J Agric Chem Environ* 2017; 06: 62–82.

[28] Leon AL, Potop GL, Hristian L, et al. Efficient technical solution for recycling textile materials by manufacturing nonwoven geotextiles. *IOP Conf Ser Mater Sci Eng* 2016; 145: 022022.

[29] Roznev A, Puzakova E, Akpedeye F, et al. Recycling in textiles. *HAMK Univ Appl Sci* 2011; 22.

[30] Scientifi O. Biodegradation of natural textile materials in Soil [Biorazgradnja naravnih tekstilnih materialov v zemlji]. *Tekstilec* 2014; 57: 118–132.

[31] Li L, Frey M and Browning KJ. Biodegradability study on cotton and polyester fabrics. *J Eng Fiber Fabr* 2010; 5: 42–53.

[32] Feller RL. *Accelerated aging: photochemical and thermal apsects*. Getty Publications, 1995.

[33] Feldman D. Polymer Weathering: Photo-Oxidation. *J Polym Environ* 2002; 10(4): 163–173.

[34] Torres FG and Nakamatsu J. Bio- and photo-degradation of natural fiber reinforced starch-based biocomposites. *Int J Polym Mater Po* 2006; 55: 893–907.

[35] Yousif E and Haddad R. Photodegradation and photostabilization of polymers, especially polystyrene: review. *Springerplus* 2013; 2: 398.

[36] Azwa ZN, Yousif BF, Manalo AC, et al. A review on the degradability of polymeric composites based on natural fibres. *Mater Des* 2013; 47: 424–442.

[37] Hablot E, Dharmalingam S, Hayes DG, et al. Effect of simulated weathering on physicochemical properties and inherent biodegradation of PLA/PHA nonwoven mulches. *J Polym Environ* 2014; 22: 417–429.

[38] Briassoulis D, Tserotas P and Hiskakis M. Mechanical and degradation behaviour of multilayer barrier films. *Polym Degrad Stab* 2017; 143: 214–230.

[39] Spiridon I, Darie-Nita RN, Hitruc GE, et al. New opportunities to valorize biomass wastes into green materials. *J Clean Prod* 2016; 133: 235–242.

[40] Jirsak O, Sadikoglu TG, Ozipek B, et al. Thermo-Insulating Properties of Perpendicular-Laid Versus Cross-Laid Lofty Nonwoven Fabrics. *Text Res J* 2000; 70: 121–128.

[41] Zhu G. Air permeability of polyester nonwoven fabrics. *Autex Res J* 2015; 15: 2–6.

[42] Liakatas A, Clark JA and Monteith JL. Measurements of the heat balance under plastic mulches. Part I. Radiation balance and soil heat flux. *Agric For Meteorol* 1986; 36: 227–239.

[43] Chevillard A, Cesar G, Gontard N, et al. Chemosphere performance and environmental impact of biodegradable polymers as agricultural mulching films. *Chemosphere* 2016; 144: 433–439.

[44] Yang Y, Ding J, Zhang Y, et al. Effects of tillage and mulching measures on soil moisture and temperature, photosynthetic characteristics and yield of winter wheat. *Agric Water Manag* 2018; 201: 299–308.

[45] Mwaikambo LY, Martuscelli E, Avellab M. Kapok/cotton fabric – polypropylene composites. *Polymer Testing* 2000; 19: 905–918.

[46] Shawe J, Riesen R, Widmann J, et al. UserCom. *Mettler Toledo* 2000; 1–28.

[47] Zhu P, Sui S, Wang B, et al. A study of pyrolysis and pyrolysis products of flame-retardant cotton fabrics by DSC, TGA, and PY-GC-MS. *J Anal Appl Pyrolysis* 2004; 71: 645–655.

[48] Macsim M, Butnaru R, Ciobanu R. Investigation of dyeing effect on the morphology of cotton fibre and cotton/PES blend by thermal analysis. Buletinul Institutului Politehnic din Iasi Publicat de Universitatea Tehnică, Gheorghe Asachi din Iaşi, Vol. LVII (LXI), pp. 54–61.

[49] Ibrahim SF, El-Amoudy ES and Shady KE. Thermal analysis and characterization of some cellulosic fabrics dyed by a new natural dye and mordanted with different mordants. *Int J Chem* 2011; 3: 40–54.

[50] Chen Q, Yang CQ and Zhao T. Heat release properties and flammability of the nylon/cotton blend fabric treated with a crosslinkable organophosphorus flame retardant system. *J Anal Appl Pyrolysis* 2014; 110: 205–212.

[51] Beg MDH and Pickering KL. Accelerated weathering of unbleached and bleached Kraft wood fibre reinforced polypropylene composites. *Polym Degrad Stab* 2008; 93: 1939–1946.

[52] Spiridon I, Leluk K, Resmerita AM, et al. Evaluation of PLA-lignin bioplastics properties before and after accelerated weathering. *Compos Part B Eng* 2015; 69: 342–349.

[53] Hayes DG, Wadsworth LC, Sintim HY, et al. Effect of diverse weathering conditions on the physicochemical properties of biodegradable plastic mulches. *Polym Test* 2017; 62: 454–467.

[54] Nguyen TX. Effects of accelerated UV exposure on mechanical properties of natural nylon, technora, and polyester fibers. *Smith Sch Work* 2017; 33–36.

[55] Skaja A, Fernando D and Croll S. Mechanical property changes and degradation during accelerated weathering of polyester-urethane coatings. *J Coat Technol Res* 2006; 3: 41–51.

[56] Brimblecombe P and Wypych G. Handbook of material weathering. *Atmospheric Environment* 1996; 39(8): 1359.

[57] Kalita H, Kamila R, Mohanty S, et al. Mechanical, thermal and accelerated weathering studies of bio-based polyurethane/clay nanocomposites coatings. *Adv Polym Technol* 2017; 37: 1–9.

[58] Kaynak C and Kaygusuz I. Consequences of accelerated weathering in polylactide nanocomposites reinforced with halloysite nanotubes. *J Compos Mater* 2016; 50: 365–375.

[59] Kijchavengkul T, Auras R, Rubino M, et al. Atmospheric and soil degradation of aliphatic-aromatic polyester films. *Polym Degrad Stab* 2010; 95: 99–107.